EFFECT OF FLUID FLOW ON INCLUSION COARSENING IN LOW-ALLOY STEEL WELDS

S. S. Babu,[*] S. A. David,[*] T. Hong,[**] and T. DebRoy[**]

[*]Metals and Ceramics Division, Oak Ridge National Laboratory, Oak Ridge, TN 37831.
[**]The Pennsylvania State University, University Park, PA 16802.

Abstract

Oxide inclusions form in welds because of deoxidation reactions in the weld pool. These inclusions control the weld microstructure development. Thermodynamic and kinetic calculation of oxidation reaction can describe inclusion characteristics such as number density, size, and composition. Experimental work has shown that fluid-flow velocity gradients in the weld pool can accelerate inclusion growth by collision and coalescence. Moreover, fluid flow in welds can transport inclusions to different temperature regions that may lead to repeated dissolution and growth of inclusions. These phenomena are being studied with the help of computational coupled heat transfer, fluid-flow, thermodynamic, and kinetic models. The results show that the inclusion formation in steel welds can be described as a function of the welding processes, process parameters, and steel composition.

DISCLAIMER

DISCLAIMER

Portions of this document may be illegible in electronic image products. Images are produced from the best available original document.

Introduction

The relationship between inclusions and formation of a high-toughness phase, namely acicular ferrite in low-alloy steel welds, is well known (1-4). Past research has focused on maximizing acicular ferrite amount in welds by controlling welding processes, process variables, and welding consumable parameters. Research has shown that there is a complex interaction between inclusion characteristics, prior austenite grain size, and weld metal hardenability. In a low-alloy steel weld, the small addition of titanium lead to a change in the inclusion composition and resulted in a transition in the microstructure from bainitic to acicular ferrite [see Fig. 1]. This in turn lead to the best combination of strength and toughness. This paper describes the inclusion formation in low-alloy steel welds.
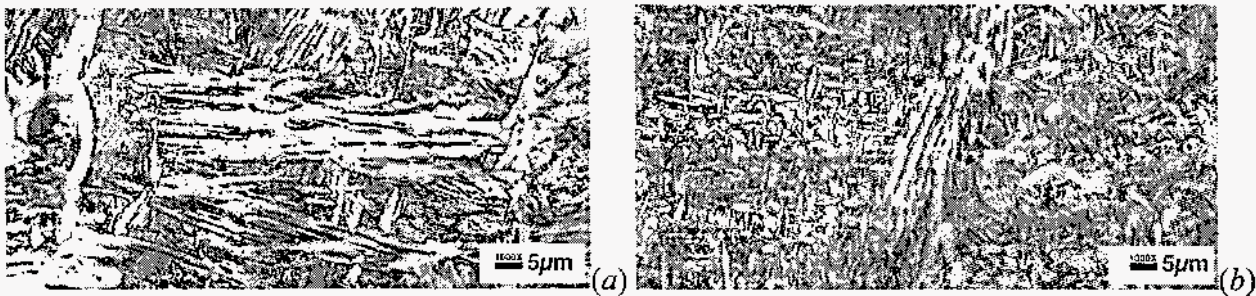

Figure 1: Optical micrographs of low-alloy steel welds showing the transition from a bainitic to an acicular ferrite microstructure with small additions of titanium (5): (a) after the addition of 7 wt.ppm of titanium and (b) after the addition of 32 wt.ppm of titanium.

Inclusion Formation in Steel Welds

Inclusions form in steel welds as a result of the reaction between dissolved aluminum, titanium, silicon, and manganese with dissolved oxygen, sulfur, and nitrogen. The inclusion characteristics such as volume fraction, size, number density, composition, and type of surface compounds have influence on the subsequent solid-state transformations. Extensive characterization of inclusions in welds has been performed (4-5). The results show that the inclusions are heterogeneous and might have formed from sequential oxidation and sulfide and nitride formation (4). Moreover, it has been observed that the inclusion characteristics are affected by welding process parameters, weld composition, and deoxidation conditions in the welding arc atmosphere. Until recently, there has been no predictive model to describe inclusion characteristics as a function of welding process parameters and composition because of its complexity. The complexity is caused by simultaneous formation of many phases (oxides, sulfides, and nitrides) during weld cooling. The kinetics of one reaction can interfere with the kinetics of the other reactions.

In the last five years, progress has been made to understand this complex inclusion formation and models have been developed to describe the inclusion formation as a function of welding process parameters [4,6-8]. In this work, oxidation kinetic equations have been extended to describe inclusion formation in steel welds, with some assumptions [4]. In the model, only simple oxides were considered. At a particular temperature, thermodynamic equilibrium between liquid steel and only one stoichiometric oxide was considered, ignoring the effects of other phases. The calculations were consistent with multicomponent thermodynamic calculations between two phases. The oxide to form first was determined by the magnitude of its driving

force for formation, ΔG, and was assumed to nucleate homogeneously. Subsequent oxides were assumed to form heterogeneously on the first oxide. To model the reactions during continuous cooling, additivity of volume fractions was assumed. The weld cooling curves were modeled using analytical equations.

The inclusion model developed with the aforementioned assumptions has been shown to be very sensitive to weld metal composition and weld cooling conditions. Evaluations of this model for a wide range of welding processes and weld cooling conditions showed its potential as a weld consumable design tool. During evaluation of inclusion formation in high-energy-density welds such as electron beam and laser beam welds, the inclusion model predicted the expected trends of increasing inclusion number density with increase in weld cooling rate [7]. However, the calculated number density did not compare well with experimental measurements. This inconsistency is attributed to the inaccuracy of analytical equations in the calculated cooling rate for electron beam and laser beam welds and can be alleviated by using computational heat transfer and fluid-flow models.

Inclusion Coarsening Caused by Collision and Coalescence

The model described previously ignored the effects of fluid flow in the weld pool. To incorporate the possible effects of fluid flow, we need to use experiments to understand the physical mechanisms. Therefore, controlled isothermal melting experiments were performed in a thermomechanical simulator [6]. In this experiment, the weld metal regions from a submerged arc (SA) steel weld were extracted and heated to a melting temperature of 1480 °C. Because of temperature gradients and current flow in the melt zone, vigorous fluid flow was induced during the isothermal coarsening experiment. Therefore, this experiment is different from the coarsening conditions in a static melt. Optical microscopy revealed rapid change in the inclusion size distribution with a holding time at 1480°C. Figure 2 compares the inclusion size distribution in the as-welded condition from the SA weld and after an isothermal hold of 60 seconds. Quantitative size distributions in the as-welded condition, after 10 and 60-s hold times, are compared in Figure 3. Results from other intermediate hold times also showed a steady increase in the inclusion size and a reduction in the number density.

The micrograph in Fig. 2 (*b*) suggests that collision and coalescence might facilitate inclusion coarsening. From the literature, it is known that such a growth will be accelerated by the presence of a fluid-flow gradient (9). Theoretical calculation of inclusion growth by collision and coalescence by Lindborg and Torssell (9) was used to examine the present results. The calculations indicate that the change in inclusion size distribution occurs rapidly in the early stages. The calculated change in inclusion size distribution compared well with the experimental measurements.

These results suggest that rapid inclusion collisions occur in welds. However, it is important to consider additional complexities caused by the spatial variation of temperature gradients, velocity gradients, and weld cooling rates. Therefore, the collision and coalescence process may be most pronounced in certain regions of the weld pool. Numerical heat transfer and fluid-flow models have to be used to describe the spatial variation of the velocity gradients in the weld pool, which are dealt with in the next section.
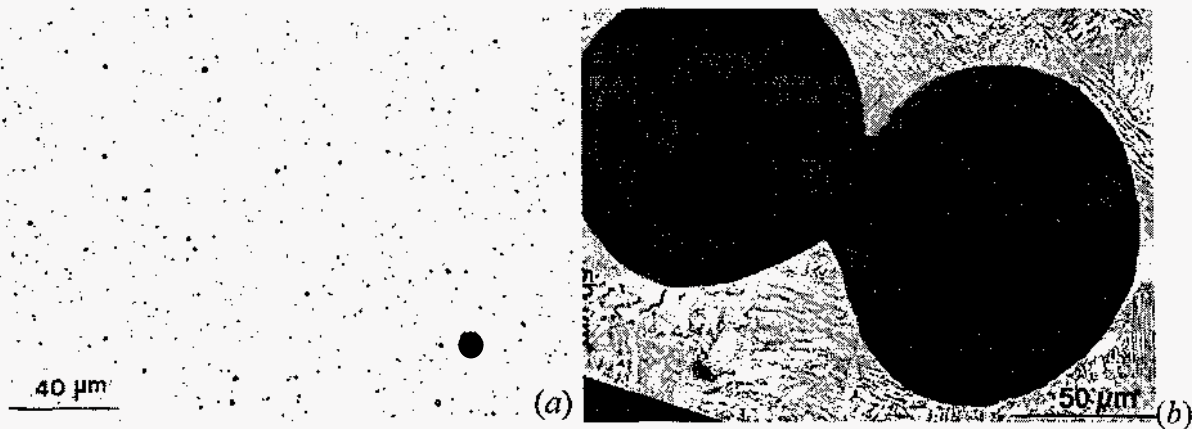
Figure 2: Comparison of inclusion size distribution with optical microscopy in the (*a*) as-welded condition and (*b*) after isothermal coarsening at 1480 °C for 60 s.
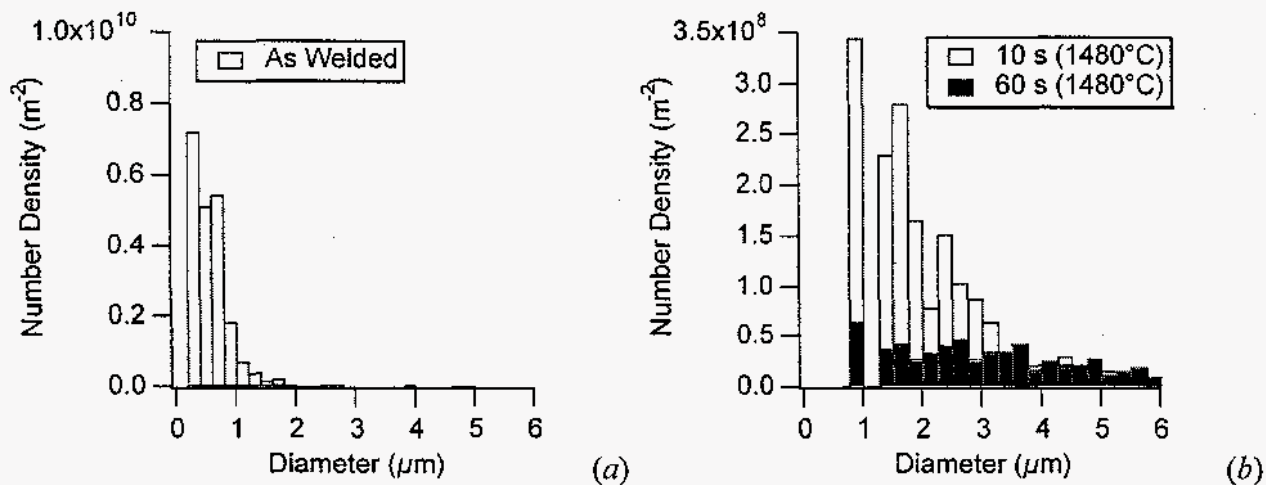

Figure 3: Comparison of inclusion size distribution measured from (*a*) as-welded condition and (*b*) after isothermal coarsening at 1480 °C for 10 s and 60 s.

Coupled Heat Transfer, Fluid Flow, and Inclusion Model

The aforementioned experimental work illustrates that we need to describe inclusion formation with computational heat transfer and fluid flow models. This will allow for predicting the nature and extent of inclusion growth caused by collision and coalescence, as well as enhanced oxide nucleation caused by local weld cooling conditions. To accomplish this task, previously developed inclusion model (4) was coupled with a generalized computational heat transfer and fluid-flow model (10).

The temperature and velocity fields and the shape and size of the weld pool are calculated using the equations of conservation of mass, momentum, and energy in three dimensions. Using the finite difference method, the coordinate system of the grid was fixed to the moving heat source. The governing equations are modified according to the fixed grid system. The details of this model are given in refs. 10 and 11.
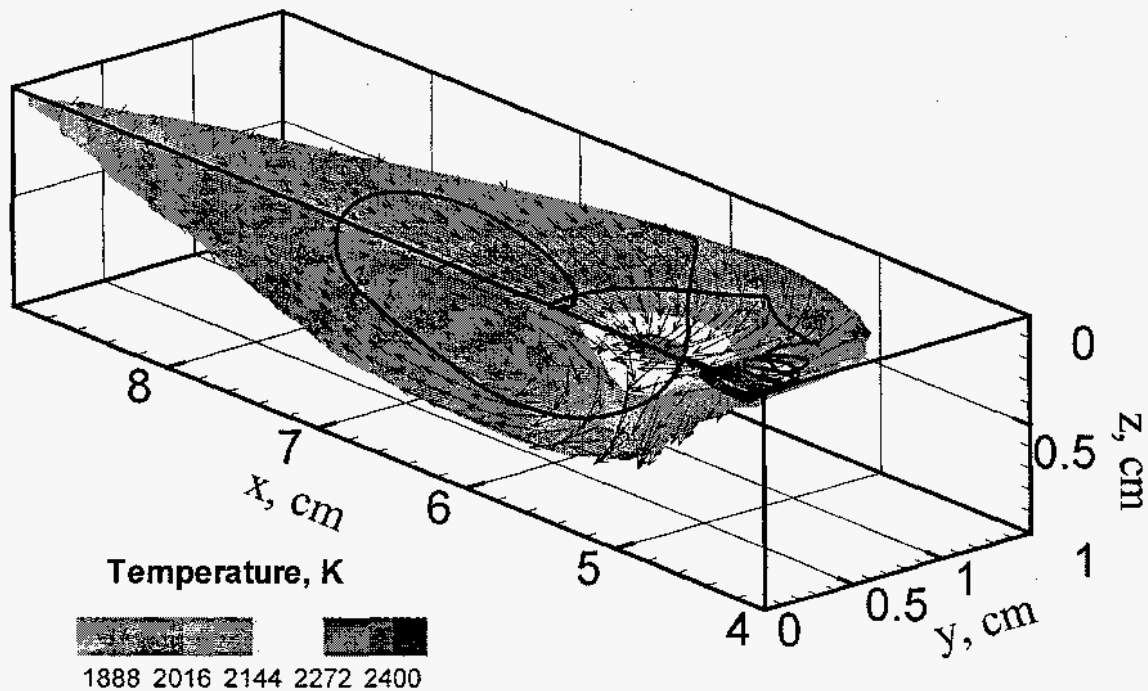
Temperature, K

1888 2016 2144 2272 2400

Figure 4: Temperature and velocity fields of the submerged arc weld pool and a typical inclusion trajectory calculated by the model.

For simplicity, only the growth and dissolution of Al_2O_3 inclusion were considered. The growth and dissolution were related to thermal excursions caused by the motion of the Al_2O_3 particles along with the fluid movement. Approximating the exact solution at a number of mesh points, starting from the initial point and moving forward, the trajectories of inclusion particles were calculated. The above model was applied to the submerged arc welding conditions given in ref. 4. The weld pool temperatures, fluid-flow vectors, and a typical inclusion trajectory are shown in Fig. 4.

Trajectories of thousands of inclusions throughout the weld metal region were calculated. The calculations yield thermal excursions experienced by these inclusions as they move through the weld pool region before they are engulfed by the solid-liquid interface. Typical temperature excursions experienced by two inclusions (A and B) at different locations are shown in Fig. 5. The plot shows, depending on the nature of thermal cycle, the inclusion may show continuous growth or repeated dissolution and growth, respectively. Thermal cycles experienced by the inclusions A and B are shown in Fig. 5. Figure 6 shows the corresponding inclusion size variation for these two inclusions. Similar calculations were repeated for many locations, and the results showed complex growth and dissolution of inclusions. In addition, the results indicated that the inclusion size is related to the residence time in the liquid steel (Fig. 7). Note that the variation of inclusion size with the cube root of residence time is similar to the behavior expected by the Ostwald ripening theory [4]. However, in these calculations the inclusion formation was described only by diffusion controlled growth and dissolution caused by thermal excursions.
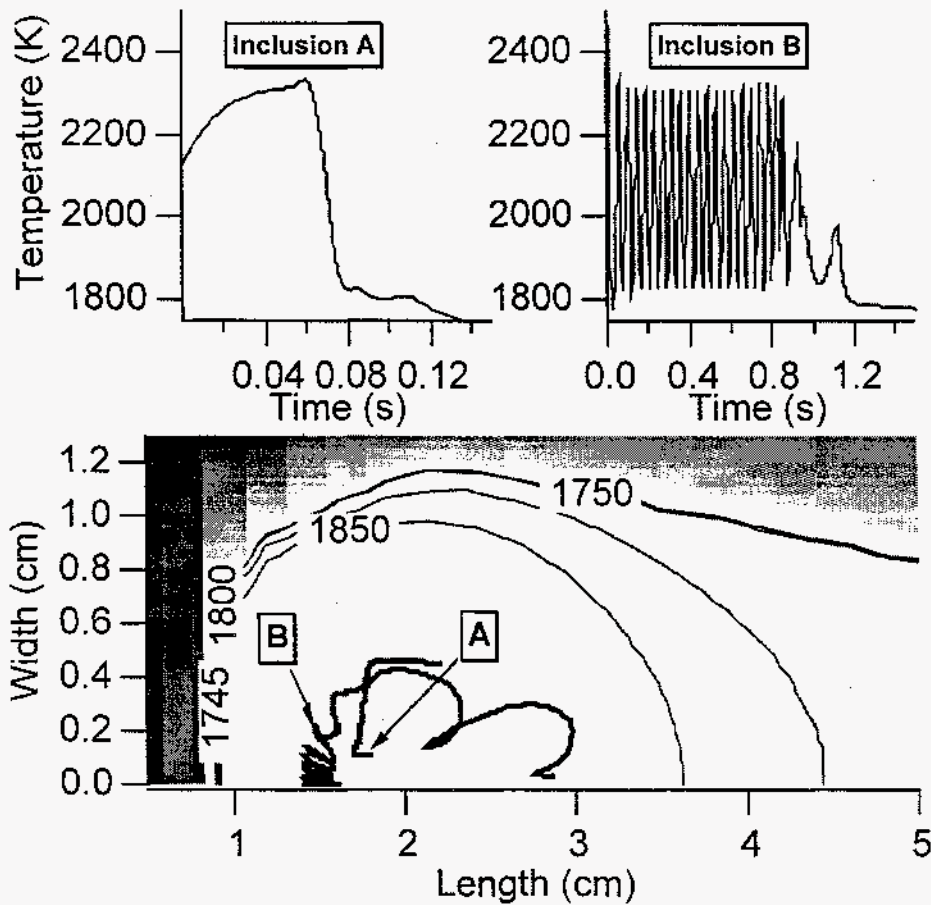
Figure 5: Top two plots compare thermal excursions and bottom plot shows surface temperature gradients and the 2-D projection of the 3-D path of two inclusions A and B predicted by the computational model.
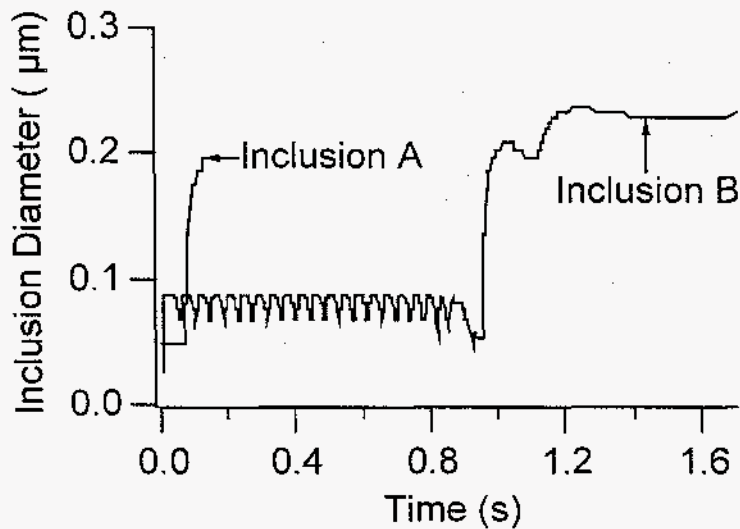

Figure 6: Comparison of inclusion growth and dissolution characteristics for inclusions A and B shown in Fig. 5.
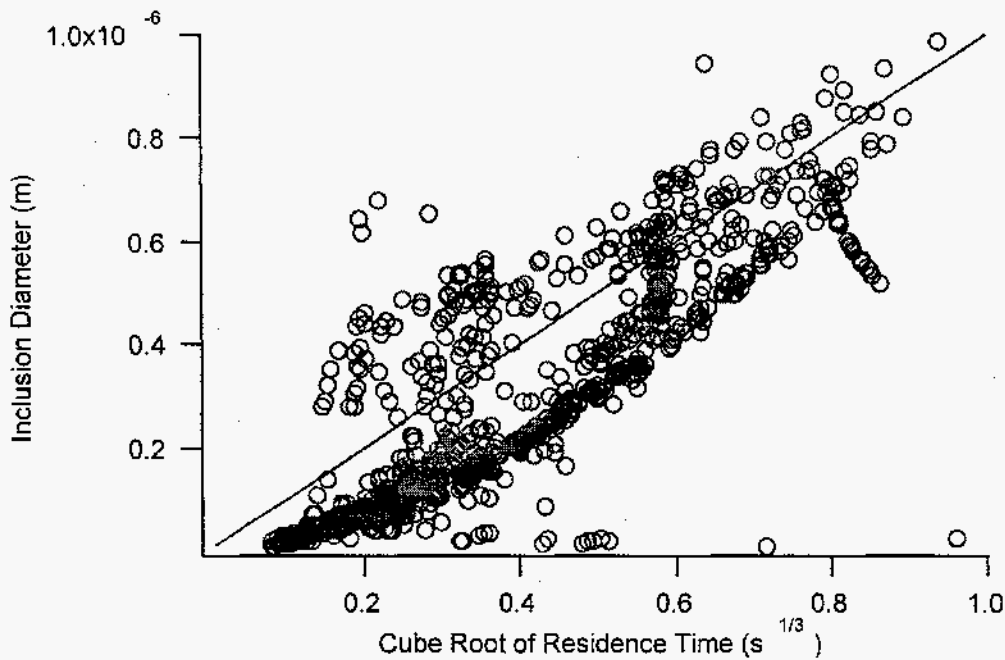
Figure 7: Diameter of thousands of inclusions as a function of the cube root of their residence time in the weld pool calculated by the computational model. The straight line in the plot shows the relation expected by the Ostwald ripening theory.

By calculating the nucleation rate for Al_2O_3 for various locations, the size distribution of the inclusions was estimated. The effect of fluid flow on the inclusion size distribution was accounted for by considering average residence time and average velocity gradients. The calculations were found to be in agreement with experimentally measured data. These calculations illustrate that it is indeed possible to quantitatively describe complex inclusion formation. Further improvements of this model are being pursued to consider other types of oxides, solidification effects, and elimination of inclusions to the slag.

Summary and Conclusions

The oxide inclusions that form in low-alloy steel welds affect microstructure development and properties. In controlled isothermal experiments, inclusion coarsening was accelerated by collision and coalescence was induced by velocity gradients.

A coupled heat transfer, fluid-flow, and inclusion model has been developed to describe the aforementioned phenomena in low-alloy steel welds as a function of weld metal composition and process parameters. The calculations show that most of the inclusions undergo complex spatial motion caused by fluid flow in the weld pool, which results in complex thermal excursions. These thermal excursions may lead to repeated growth, dissolution, and collision and coalescence of inclusions.

Acknowledgements

References

1. Y. Ito, M. Nakanishi, and Y. Komizo, "Study on charpy impact properties of weld metals with submerged arc welding," Sumitomo Search, 15 (1976), 42-62.

2. S. Liu and D. L. Olson, "The role of inclusions in controlling HSLA steel weld microstructures," Welding Journal, 65 (1986) 139s-149s.

3. Φ. Grong and D. K. Matlock, "Microstructural development in mild and low alloy steel weld metals," Int. Met. Reviews, 31 (1986) 27-48.

4. S. S. Babu et al., "Development of macro – and microstructures of C–Mn low alloy steel welds – Inclusion Formation," Mater. Sci. Technol., 11 (1995) 186-199.

5. G. M. Evans and N. Bailey, Metallurgy of Basic Weld Metals, (Cambridge, England: Abington Publishing, 1997), 391-420.

6. S. S. Babu, S. A. David, and T. DebRoy, "Coarsening of oxide inclusions in low alloy steel welds," Sci. Tech. Weld. Join., 1 (1996) 17-27.

7. S. S. Babu et al., "Effect of high-energy-density welding processes on inclusion and microstructure formation in steel welds," Sci. Tech. Weld. Join., 1 (1998) accepted for publication.

8. T. Hong, W. Pitscheneder, and T. DebRoy: "Quantitative Modeling of Inclusion Growth in the Weld Pool by Considering their Motion and Temperature Gyrations", Science and Technology of Welding and Joining, 3 (1) (1998) 33-41.

9. U. Lindborg and K. Torssell, "A collision model for the growth and separation of deoxidation products," Trans of the Metallurgical society of AIME, 242 (1968) 94-102.

10. K. Mundra, T. DebRoy, and K. M. Kellkar, "Numerical predication of fluid flow and heat transfer in welding with a moving heat source," Numerical Heat Transfer, Part A, 29 (1996) 115-129.

11. W. Pitscheneder et al. "Experimental and numerical investigation of transport phenomena in conduction mode weld pools," (Paper presented at the 3rd Inter. Seminar on Numerical Analysis of Weldability, Graz, Austria, 1997).